SCIENCE CHINA
Chemistry

• ARTICLES •

December 2011 Vol.54 No.12: 1955–1961
doi: 10.1007/s11426-011-4413-9

Correlation between the molecular structure and *trans* ↔ *cis* isomerization characteristics of azobenzenes

HAN Mina[*] & HONDA Takumu

Department of Chemistry and Department of Electronic Chemistry,
Tokyo Institute of Technology, 4259 Nagatsuta, Midori-ku, Yokohama 226-8502, Japan

Received August 17, 2011; accepted September 15, 2011

Photochemical and thermal isomerization of various azobenzenes was systematically investigated to understand the correlation between the molecular structure and *trans* ↔ *cis* isomerization characteristics of azobenzenes. A blue shift in π–π^* absorption band of ortho-alkylated azobenzenes (**1o** and **2o**) was observed together with a reduction in molar extinction coefficient (ε) in comparison with both meta-alkylated azobenzenes (**4m** and **5m**) and **7p** lacking the meta and ortho substituents. For ortho-alkylated azobenzene, photochemical *trans*-to-*cis* isomerization and thermal back *cis*-to-*trans* isomerization in solution occurred slowly when compared with **4m**, **5m** and **7p**. The half-life time of the *cis* form of **2o** was found to be 380 h, which is about 8–50 times longer than those of comparable **4m**, **5m** (43–13 h) and **7p** (7 h). Furthermore, comparison of the molecular structure and isomerization characteristics of azobenzene thiol (**2o** and **5m**) self-assembled monolayers on flat gold surfaces indicates that the *trans*-to-*cis* photoconversion in monolayer systems is influenced by steric hindrance and strong intermolecular interaction between azobenzene units.

azobenzene, isomerization, lifetime of *cis* form, molecular structure

1 Introduction

Photochromic azobenzene molecules undergo *trans*-to-*cis* isomerization upon irradiation with UV light and this process can be reversed by either heating or irradiation with visible light [1–7]. The *trans* form is thermodynamically more stable by about 12 kcal mol^{-1} than the *cis* form, and the *cis* form is kinetically stabilized by an activation barrier of isomerization. There are two possible isomerization mechanisms in azobenzene: via rotation of the phenyl ring about the N=N bond or in-plane inversion around one of the nitrogen atoms [1–9]. Experimental data and theoretical calculations predominantly support the inversion mechanism for thermal isomerization of both the parent azobenzene and its substituted azobenzene derivatives [10–14].

In general, thermal *cis*-to-*trans* isomerization occurs on the time scale of minutes to hours and the lifetime of the *cis* form is influenced by the surrounding environment (solvents, polymer matrix, temperature, etc.) as well as the molecular structure [15–23]. In particular, the steric factor in azobenzene can significantly vary the rate of thermal *cis*-to-*trans* isomerization. As an example the steric strain in azobenzenophanes, in which two azobenzenes are cyclically connected by relatively short atomic chains, influences the lifetime of the *cis* form, from seconds to years [24–28]. Tamaoki *et al.* have reported that the lifetime of the *cis*-*cis* isomer in a xanthene-based cyclic azobenzene dimer was increased up to 6.4 years, and that an azobenzenophane, an azobenzene dimer connected at 3- and 3′-positions without spacers, formed thermodynamically stable *cis* form [27, 28].

Other sterically hindered azobenzene molecules are produced by introducing bulky substituents to the benzene ring [29, 30]. Wheeler and Gore have reported the results of spectroscopic investigation of ortho- and para-substituted azobenzenes [31]. Bunce *et al.* have also showed spectro-

---

[*] Corresponding author (email: han.m.ab@m.titech.ac.jp)

scopic data and the results of quantum mechanical calculations for a series of azobenzenes [32, 33]. Despite these investigations, systematic information regarding photochemical and thermal isomerization of ortho-, meta-, and para-substituted azobenzenes in solution as well as in monolayers is desirable. Here we prepared ortho- (**1o** and **2o**) and meta-alkylated (**4m** and **5m**) azobenzenes, and **7p** lacking the meta and ortho substituents (Scheme 1) to clarify the relationship between the molecular structural and spectroscopic features. Photochemical and thermal isomerization as well as the related thermodynamic parameters was also investigated to obtain insight into molecular structure factors responsible for controlling *trans* ↔ *cis* isomerization and the lifetime of the *cis* form. Furthermore, we examined reversible photoswitching of the molecular conformation in self-assembled monolayers (SAMs) on a flat gold surface.

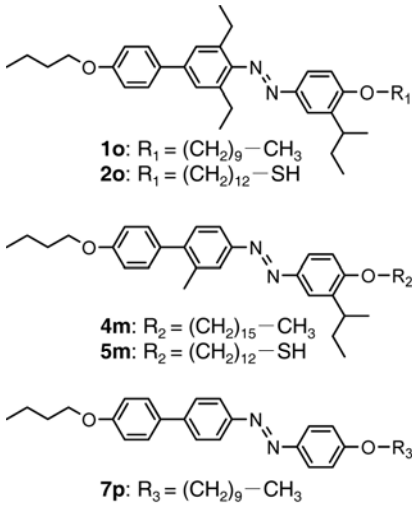

Scheme 1 Molecular structures of **1o**–**2o**, **4m**–**5m** and **7p**.

2 Experimental section

2.1 Instrumentation

Dimethylformamide (DMF) and dichloromethane (DCM) of spectroscopic grade were used to dissolve the azobenzenes. Azobenzene solutions were exposed to UV light (365 nm, 1–2 mW cm^{-2}, Mineralight® lamp, Model UVGL-25) or visible light (436 nm, 1–2 mW cm^{-2}, a high-pressure UV lamp, Ushio Inc., combination of Toshiba color filters, Y-43+V-44). Absorption spectra were recorded on a Shimadzu UV-3100PC UV-vis-NIR scanning spectrophotometer. NMR spectra were obtained using JEOL JNM-EX270 (270 MHz) and JEOL JNM-ECP300 (300 MHz) spectrometers.

2.2 Synthesis

All azobenzenes (including **2o** and **5m** [34]) were synthesized according to the procedure in the literature [35, 36].

*(E)-1-(4′-butoxy-3,5-diethylbiphenyl-4-yl)-2-(4-(decyloxy)-3-isopropylphenyl)diazene (**1o**)*

1o was prepared by reacting (*E*)-4-((4′-butoxy-3,5-diethylbiphenyl-4-yl)diazenyl)-2-*sec*-butylphenol (3.00 g, 6.5 mmol) with 1-bromodecane (4.33 g, 19.6 mmol) in 60 mL acetone in the presence of K_2CO_3 (2.71 g, 19.6 mmol) and a catalytic amount of tetrabutylammonium bromide. The reaction mixture was stirred at 60 °C for 7 h and then cooled to room temperature, followed by addition of water and ethyl acetate. The organic layer was collected and the solvent was evaporated. The residue was purified by silica gel column chromatography (hexane : dichloromethane, *v*/*v* = 3/1).

Yield: 55%. ^{1}H NMR (270 MHz, $CDCl_3$, ppm) δ 0.88 (t, 3H, C*H*$_3$), 0.99 (t, 3H, C*H*$_3$), 1.1–1.6 (m, 28H, C*H*$_2$ and C*H*$_3$), 1.82 (m, 4H, C*H*$_2$), 2.74 (q, 4H, ArC*H*$_2$C*H*$_3$), 3.37 (m, 1H, ArC*H*), 4.02 (tt, 4H, ArOC*H*$_2$), 6.94 (m, 3H, Ar-*H*), 7.31 (s, 2H, Ar-*H*), 7.53–7.83 (m, 4H, Ar-*H*). ^{13}C NMR (300 MHz, $CDCl_3$) 13.9, 14.1, 15.6, 19.3, 22.4, 22.7, 25.4, 26.2, 27.2, (–CH$_2$–; 29.72, 29.31, 29.54, 29.57), 31.3, 31.9, 67.8, 68.3, 110.9, 114.7, 120.4, 122.1, 125.8, 128.1, 133.4, 136.8, 137.8, 140.0, 147.0, 150.1, 158.7, 159.1. Anal. calcd: C, 80.09%; H, 9.65%; N, 4.79%. Found: C, 80.03%; H, 9.75%; N, 4.72%. FAB-MS (*m*/*z*): [M+H]$^+$ found 585, calcd for $C_{39}H_{56}N_2O_2$ = 584.43.

*(E)-1-(4′-butoxy-2-methylbiphenyl-4-yl)-2-(3-sec-butyl-4-(hexadecyloxy)phenyl)diazene (**4m**)*

^{1}H NMR (270 MHz, $CDCl_3$) δ 0.81 (m, 6H, C*H*$_3$), 0.90 (t, 3H, *CH*$_3$), 1.2–1.8 (m, 37H, C*H*$_2$ and C*H*$_3$), 2.30 (s, 3H, ArC*H*$_3$), 3.10 (m, 1H, ArC*H*), 3.96 (tt, 4H, ArOC*H*$_2$), 6.84–6.90 (m, 3H, Ar-*H*), 7.18–7.28 (m, 3H, Ar-*H*), 7.64–7.75 (m, 4H, Ar-*H*). ^{13}C NMR (300 MHz, $CDCl_3$) 12.3, 13.9, 14.1, 19.3, 20.3, 20.7, 22.7, 26.1, (–CH$_2$–; 29.28, 29.33, 29.35, 29.58, 29.65, 29.66, 29.69, 29.77), 31.4, 31.9, 33.9, 67.7, 68.3, 111.0, 114.1, 120.0, 121.8, 122.0, 124.2, 130.2, 130.6, 133.5, 136.3, 136.7, 143.6, 146.8, 151.8, 158.4, 159.2. Anal. calcd: C, 80.57%; H, 10.06%; N, 4.37%. Found: C, 80.21%; H, 10.16%; N, 4.39%. FAB-MS (*m*/*z*): [M+H]$^+$ found 641, calcd for $C_{43}H_{64}N_2O_2$ = 640.50.

*(E)-1-(4′-butoxybiphenyl-4-yl)-2-(4-(decyloxy)phenyl)diazene (**7p**)*

Yield: 45%. ^{1}H NMR (300 MHz, $CDCl_3$) δ 0.89 (t, 3H, C*H*$_3$), 0.99 (t, 3H, C*H*$_3$), 1.1–1.7 (m, 16H, C*H*$_2$), 1.82 (m, 4H, C*H*$_2$), 4.04 (tt, 4H, ArOC*H*$_2$), 6.97 (m, 4H, Ar-*H*), 7.58 (d, 2H, Ar-*H*), 7.67 (d, 2H, Ar-*H*), 7.91 (m, 4H, Ar-*H*). Anal. calcd: C, 78.97% ; H, 8.70%; N, 5.76%. Found: C, 78.81%; H, 8.63%; N, 5.75%. FAB-MS (*m*/*z*): [M + H]$^+$ found 488, calcd for $C_{32}H_{43}N_2O_2$ = 487.33.

3 Results and discussion

The photophysical data corresponding to the azobenzenes used in this study are presented in Table 1. Varying the substituents at one end of the tail part for the same azobenzene unit (**1o**–**2o** and **4m**–**5m**) has little effect on the transition bands in UV-vis absorption spectra; that is, strong spectral overlap between the bands can be seen in Figure 1. The series of meta-methylated azobenzenes in dichloromethane (DCM) possessed strong π–π^* absorption bands at 368 nm and negligibly weak n–π^* bands in the as-prepared *trans*-rich state. The $\lambda_{\max}$ of π–π^* absorption band at 354 nm of ortho-alkylated azobenzenes showed a blue shift, together with a considerable reduction of about 30%–40% in molar extinction coefficient (ε), in comparison with those of **4m**–**5m** and **7p** (Table 1) [37].

The observed spectroscopic features are closely related to the steric effect arising from the substitution of two ethyl groups at the ortho positions with respect to the azo group. It is known that unsubstituted *trans*-azobenzene adopts a planar conformation, and that methyl substituents even at the ortho positions have little influence on the planar structure of azobenzene in the crystal state [13, 38]. By contrast, our X-ray crystal structure analysis revealed that the introduction of two ethyl groups at the ortho positions led to a large distortion of the phenyl ring from coplanarity [35, 39].

3.1 Photochemical *trans*-to-*cis* isomerization

Figure 2 shows typical examples of changes in the absorbance at $\lambda_{\max}$ during *trans*-to-*cis* isomerization of the azobenzenes as a function of 365 nm light irradiation time. UV light irradiation for 6 min caused sufficient *trans*-to-*cis* isomerization for **5m**, as shown with the significant reduction in π–π^* absorption band. By contrast, **2o** reached a *cis*-rich photostationary state within 10 min of UV light irradiation and showed slower *trans*-to-*cis* isomerization. More than 95% of the *cis* form for all azobenzenes was generated at a photostationary state of UV light irradiation, as confirmed by NMR and UV-vis absorption spectroscopy measurements.

Table 1 Photophysical data of azobenzenes in dichloromethane (DCM)

Cpd	π–π^* (nm) ε (L mol^{-1} cm^{-1})	n–π^* (nm) ε (L mol^{-1} cm^{-1})$^{a)}$	$t_{1/2}$ (h)$^{b)}$
1o	353.5 (25,000)	448 (2,000)	–$^{c)}$
2o	354 (26,000)	449 (2,100)	380
4m	368 (36,000)	447.5 (3,400)	43
5m	368 (37,000)	447 (3,400)	13
7p	373 (41,000)	450 (4,200)	7

a) After UV light irradiation (*cis*-rich state); b) at 293 K; c) not determinable.

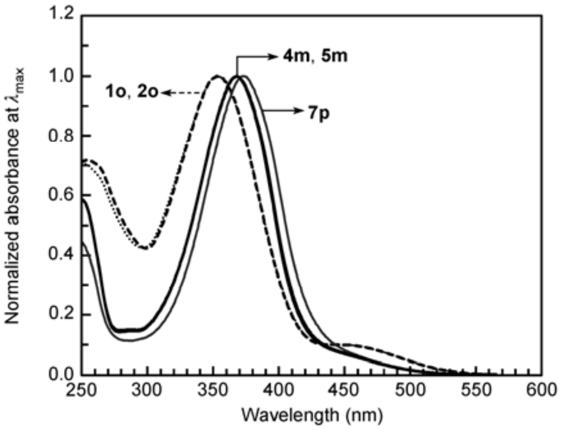

Figure 1 UV-vis absorption spectra of as-prepared azobenzenes (**1o**–**2o**, **4m**–**5m** and **7p**) in DCM.

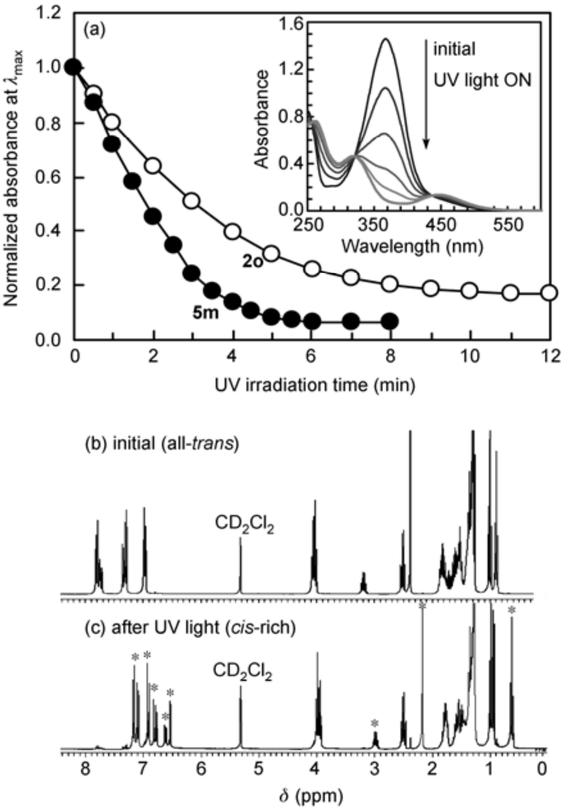

Figure 2 (a) Changes in the normalized absorbance at $\lambda_{\max}$ as a function of 365 nm light irradiation time. Inset: changes in absorption spectra of **5m** in DCM. ^{1}H NMR spectra of (b) all-*trans* **5m** and (c) after UV light irradiation.

3.2 Photochemical and thermal *cis*-to-*trans* isomerization

Reverse *cis*-to-*trans* isomerization can be induced either photochemically or thermally. First, upon irradiation of the UV-exposed solution with visible light at 436 nm, the π–π^* absorption band was increased up to about 70% with respect to the initial π–π^* absorbance (Figure 3). This result indicates that about 30% of the *cis* form still existed in the photostationary state of visible light [40]. Further alternating UV and visible light irradiation caused reversible *trans*-to-*cis* and *cis*-to-*trans* isomerization processes, reaching respective

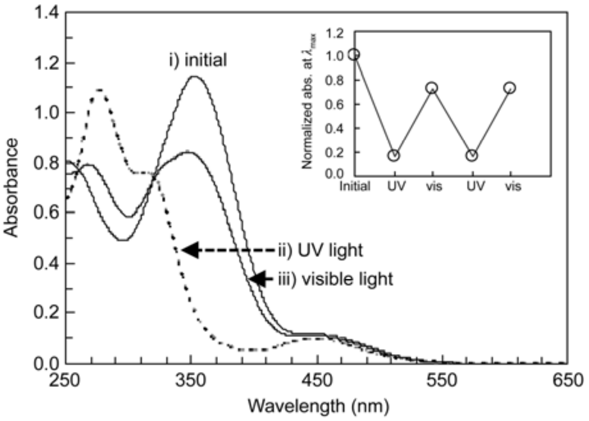

Figure 3 Changes in absorption spectra of **2o** in DCM. Inset: Normalized absorbance at $\lambda_{\max}$ upon alternating UV and visible light irradiation.

photostationary states of UV and visible light.

Second, dark incubation of the UV-exposed solution resulted in a slow maximization of π–π* absorption band as a consequence of thermal *cis*-to-*trans* isomerization, which followed the first-order kinetics according to the following equation:

$$\ln\left\{\frac{A_o - A_\infty}{A_t - A_\infty}\right\} = kt$$

where A_o, A_∞, and A_t are the absorbance at $\lambda_{\max}$ of π–π* band of *trans*-azobenzene, before exposure to UV light, at a photostationary state of UV light, and at time t, respectively. k is the first-order rate constant for thermal *cis*-to-*trans* isomerization. The absorbances are substantially proportional to the concentrations of the *trans* form at the monitoring wavelength and the ratio of the *trans* form was corrected based on NMR data. Obviously, thermal back *cis*-to-*trans* isomerization of the sterically hindered **2o** proceeded much more slowly at room temperature and the half-life time of **2o** (380 h) was approximately 8–50 times longer than those of the comparable **4m**–**5m** (43–13 h) and **7p** (7 h), as shown in Figure 4 and Table 1. Such slow isomerization rate of **2o** is due to bulky substituents that inhibit large-scale distortion of the azo group for *trans* ↔ *cis* isomerization [33]. Further evidence for *trans* ↔ *cis* isomerization was provided by NMR experiments (Figure 5). Approximately 50% of *cis*-to-*trans* conversion of **2o** took place after about 2 weeks in the dark and approximately 3%–5% of the *cis* form still existed in solution after 2 months, consistent with UV-vis absorption spectroscopic data.

Calculation of the first-order rate constant at the various temperatures allowed us to estimate thermodynamic activation parameters such as the activation energy (E_a), activation enthalpy ($\Delta H^{\ddagger}$), and activation entropy ($\Delta S^{\ddagger}$) for thermal *cis*-to-*trans* reaction from Arrhenius and Eyring plots. Figure 6 shows the first-order plot for thermal *cis*-to-*trans* isomerization of **2o** in DMF. The evaluated values for **2o** and **5m**, and **7p** in DMF and DCM are listed in Table 2. The preexponential factor, $A_{\mathbf{2o}}$, was one order larger in magnitude and the corresponding activation entropy ($\Delta S^{\ddagger}_{\mathbf{2o}}$) was less negative (faster component) when compared with those for **5m** and **7p**. On the other hand, the activation energies of ortho-alkylated **2o** were about 2–4 kcal mol^{-1} higher than those of **5m** and **7p** in solution ($E_{a(\mathbf{2o})} > E_{a(\mathbf{5m})} > E_{a(\mathbf{7p})}$).

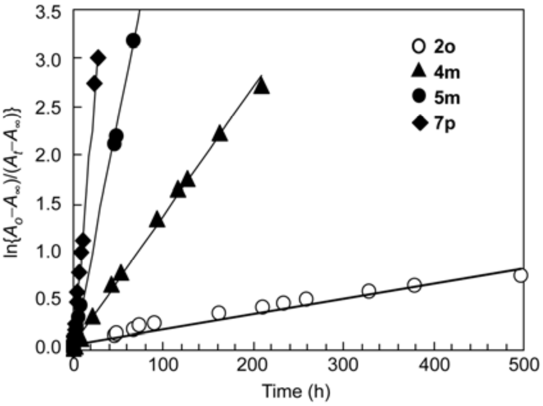

Figure 4 First-order plots for thermal *cis*-to-*trans* isomerization of azobenzenes in DCM at 20 °C.

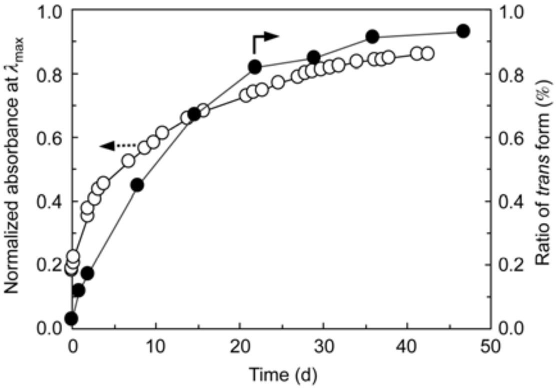

Figure 5 Changes in the normalized absorbance at $\lambda_{\max}$ of π–π* band (○) of **2o**, and the ratio of the *trans* form (●) of **2o** obtained from ^{1}H NMR experiments as a function of dark incubation time at ambient temperature.

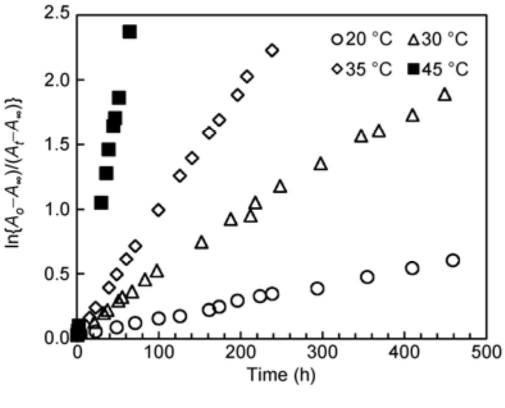

Figure 6 First-order plots for thermal *cis*-to-*trans* isomerization of **2o** in DMF at various temperatures.

Table 2 Thermodynamic activation parameters of thermal *cis*-to-*trans* isomerization of **2o**, **5m** and **7p**

Cpd	DCM				DMF			
	A (s^{-1})	E_a (kcal mol^{-1})	$\Delta H^\ddagger$ (kcal mol^{-1})	$\Delta S^\ddagger$ (cal K^{-1} mol^{-1})	A (s^{-1})	E_a (kcal mol^{-1})	$\Delta H^\ddagger$ (kcal mol^{-1})	$\Delta S^\ddagger$ (cal K^{-1} mol^{-1})
2o	2.3×10^{11}	23.8	23.2	−8.5	2.6×10^{11}	23.9	23.4	−8.3
5m	0.14×10^{11}	20.4	19.8	−13.4	0.93×10^{11}	21.6	21.1	−10.3
7p	0.065×10^{11}	19.4	18.8	−15.6	0.81×10^{11}	20.9	20.3	−10.7

Figure 7 shows isokinetic plots for $\Delta H^\ddagger$ and $\Delta S^\ddagger$ based on the rate constants at various temperatures for azobenzenes so as to evaluate the mechanism of thermal isomerization. All the plots for **2o**, **5m**, and **7p** in different solvents are around the straight line including azobenzenes known to isomerize through the inversion mechanism [11, 13, 29]. Steric hindrance arising from additional substitutions at the meta and ortho positions did not cause a large deviation from the linear relationship. Our data thus suggest that isomerization for the azobenzenes used in this study proceeds through the inversion mechanism rather than the rotation mechanism requiring a larger volume change, irrespective of substituents attached to azobenzene units.

3.3 Photoresponsive azobenzene-based self-assembled monolayers (SAMs)

We fabricated SAMs of azobenzene thiols (**2o** and **5m**) to investigate the photoresponse of azobenzene units chemisorbed on flat gold surfaces. Azobenzene SAMs were prepared by immersion of sold substrates in azobenzene solution in DCM for 1–2 days. After immersion, the sample was rinsed with DCM, and blown dry with nitrogen gas [34, 36, 41]. Single-component azobenzene thiol generated a homogeneously distributed smooth monolayer with the root-meansquare surface roughness of 1.6±0.2 Å. The contact angles of **2o** and **5m** SAMs for water on a flat gold substrate were 94°±1° and 94.6°±1°, respectively. The π–π^* absorption band at 350 nm of ortho-alkylated **2o** monolayer was similar to that ($\lambda_{\max}$ = 354 nm) of the monomer-like absorption spectrum in solution (Figure 8(a)). By contrast, the π–π^* absorption band of **5m** monolayer was substantially blue-shifted (Figure 8(b)), which is explained in terms of H-aggregation through strong intermolecular interaction between planar **5m** azobenzene units.

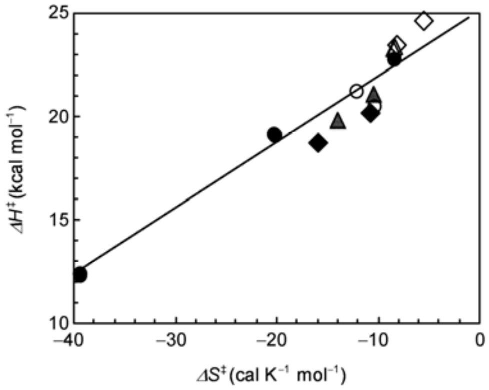

Figure 7 Isokinetic plots for $\Delta H^\ddagger$ and $\Delta S^\ddagger$ of thermal isomerization of azobenzenes. **2o** (△); **5m** (▲); **7p** (◆); unsubstituted azobenzene in different solvents [11, 13] (○); para-substituted azobenzene [11] (●); ortho-alkylated azobenzenes [29] (◇).

UV light irradiation caused the significant decrease in the π–π^* absorption band and emergence of a band at around 280 nm (Figure 8(a)). The *trans*-to-*cis* photoconversion was found to be ~90% for sterically hindered **2o** SAMs, almost identical to those obtained with **2o** dissolved in solution, strongly indicative of reversible photoswitching of the molecular conformation between the *trans* and *cis* forms in monolayer systems. Despite the high *trans*-to-*cis* photoisomerization, the molecular photoswitches in smooth azobenzene thiol monolayers could hardly be visualized by atomic force microscopy.

On the other hand, the estimated *trans*-to-*cis* photoconversion yield of **5m** SAMs was about 50%, even though the area-per-molecule value is improved by the introduction of alkyl groups at the meta position. UV light irradiation for 10–15 min decreased the contact angle to 91° from 94.6° (Figure 8(c)). The contact angle did not increase to a higher value after the first visible-light irradiation. Upon the second UV light irradiation, the contact angle on the SAM was decreased to ~87°. This behavior might be associated with the relatively low photoconversion and strong molecular interactions between the planar azobenzene units.

Thermal *cis*-to-*trans* isomerization of **5m** SAM proceeded over 2 h at ambient temperature. The kinetics of the photoisomerization reaction was characterized by use of the first-order plot. As shown in Figure 8(d), the *cis*-to-*trans* isomerization deviated from the linearity predicted by the first-order, suggesting the strong tendency to form H-aggregates between **5m** molecules in monolayers. Nevertheless, the origin of difference in the thermal *cis*-to-*trans* isomerization rate between in monolayer and in solution still remains to be solved.

4 Conclusions

The spectroscopic features and *trans* ↔ *cis* isomerization behavior of ortho-ethylated azobenzenes (**1o** and **2o**) were investigated in comparison with meta-methylated azobenzenes (**4m** and **5m**) and **7p** lacking the meta and ortho substituents. In contrast to **4m**, **5m** and **7p**, the sterically hindered **1o** and **2o** undergo distortion of the phenyl ring in the

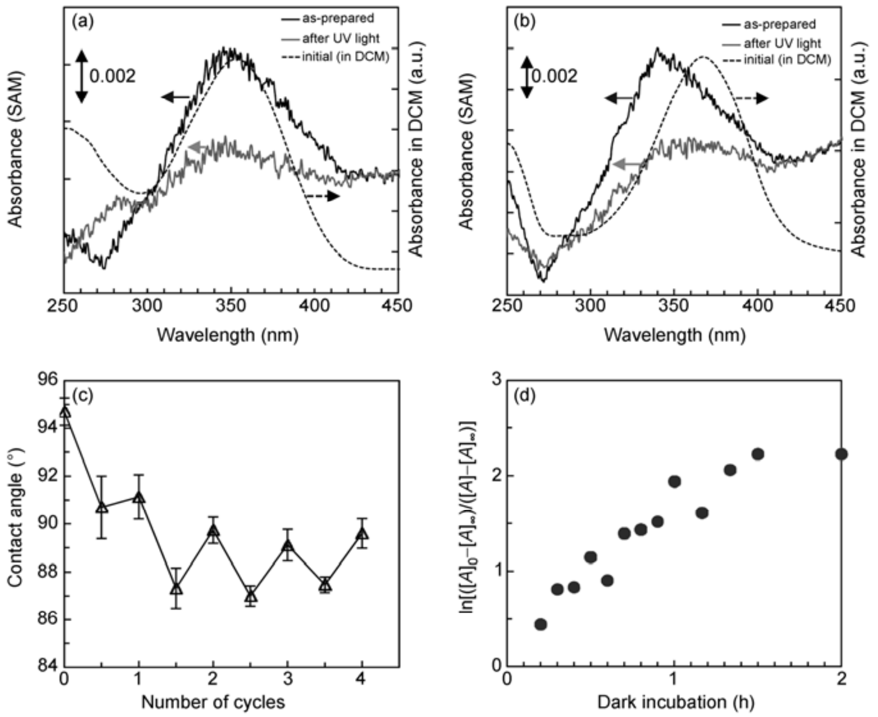

Figure 8 UV-vis absorption spectral changes of (a) **2o** and (b) **5m** SAMs on gold substrates; (c) changes of the water contact angle of **5m** SAM as a function of photoirradiation during four cycles; (d) first-order plot for thermal *cis*-to-*trans* isomerization of **5m** in SAM.

azobenzene unit from coplanarity, which is likely responsible for spectroscopic features (such as a blue shift in π–π^* absorption bands and a reduction in the molar extinction coefficient). Photochemical and thermal isomerization rates and the lifetime of the *cis* form showed obvious dependence on the molecular structure of azobenzene. For **2o** slow thermal isomerization was found when compared with **4m**, **5m** and **7p**. The experimental results for thermal isomerization indicate that the inversion mechanism is predominantly operative in the azobenzenes, irrespective of additional substituents attached to the azobenzene unit. Furthermore, SAMs of sterically hindered azobenzene thiols showed the reversible photoswitching nature on gold surface. Our investigation suggests that understanding the correlation between the molecular structure and isomerization characteristics provides insight into the molecular design strategy for controlling photochemical and thermal isomerization behaviors.

We are grateful to the Center for Advanced Materials Analysis (Suzukakedai), Technical Department, Tokyo Institute of Technology, for FAB-MS and elemental analyses. This work was supported by the Global COE Program from the Ministry of Education, Culture, Sports, Science, and Technology of Japanese Government.

1 Dürr H, Bouas-Laurent H. *Photochromism*: *Molecules and Systems*. Amsterdam: Elsevier, 1990
2 Zollinger H. *Color Chemistry: Synthesis, Properties and Applications of Organic Dyes and Pigments*, 2nd eds. Weinheim: VCH, 1991
3 Ichimura K. Photoalignment of liquid-crystal systems. *Chem Rev,* 2000, 100: 1847–1873
4 Pieroni O, Fissi A, Angelini N, Lenci F. Photoresponsive polypeptides. *Acc Chem Res,* 2001, 34: 9–17
5 Dugave C, Demange L. *Cis-trans* isomerization of organic molecules and biomolecules: Implications and applications. *Chem Rev,* 2003, 103: 2475–2532
6 In: Sekkat Z, Knoll W, eds. *Photoreactive Organic Thin Films*. New York: Academic Press, Elsevier Science, 2002
7 Ishi-i T, Shinkai S. Dye-based organogels: Stimuli-responsive soft materials based on one-dimensional self-assembling aromatic dyes. *Top Curr Chem*, 2005, 258: 119–160
8 Rau H. Spectroscopic properties of organic azo-compounds. *Angew Chem Int Ed Engl*, 1973, 12: 224–235
9 Cembran A, Bernardi F, Garavelli M, Gagliardi L, Orlandi G. On the mechanism of the *cis-trans* isomerization in the lowest electronic states of azobenzene: S-0, S-1, and T-1. *J Am Chem Soc*, 2004,126: 3234–3243
10 Shinkai S, Nakaji T, Nishida Y, Ogawa T, Manabe O. Photoresponsive crown ethers.1. *Cis-trans* isomerism of azobenzene as a tool to enforce conformational-changes of crown ethers and polymers. *J Am Chem Soc*, 1980, 102: 5860–5865
11 Asano T, Okada T, Shinkai S, Shigematsu K, Kusano Y, Manabe O. Temperature and pressure dependences of thermal *cis*-to-*trans* isomerization of azobenzenes which evidence an inversion mechanism. *J Am Chem Soc*, 1981, 103: 5161–5165
12 Rau H, Lüddecke E. On the rotation-inversion controversy on photo-isomerization of azobenzenes. Experimental proof of inversion. *J Am Chem Soc*, 1982, 104: 1616–1620
13 Ruslim C, Ichimura K. Spectroscopic and thermal isomerization characteristics of 3,3′-dialkoxy and dialkanoyloxy azobenzenes. *J Mater Chem*, 2000, 10: 2704–2707
14 Sokalski WA, Gora RW, Bartkowiak W, Kobylinski P, Sworakowski J, Chyla A, Leszczynski J. New theoretical insight into the thermal *cis-trans* isomerization of azo compounds: Protonation lowers the activation barrier. *J Chem Phys*, 2001, 114: 5504–5508 and references therein
15 Irick G, Pacifici JG. Photochemistry of azo compounds. I. Photoreduction of 4-diethylamino-4′-nitroazobenzene. *Tetrahedron Lett*, 1969, 10: 1303–1306
16 Wildes PD, Pacifici JG, Irick G, Whitten DG. Solvent and substituent effects on thermal isomerization of substituted azobenzenes. Flash spectroscopic study. *J Am Chem Soc*, 1971, 93: 2004–2008

17 Gabor G, Fischer E. Spectra and *cis-trans* isomerism in highly bipolar derivatives of azobenzene. *J Phys Chem*, 1971, 75: 581–583

18 Paik CS, Morawetz H. Photochemical and thermal isomerization of azoaromatic residues in side chains and backbone of polymers in bulk. *Macromolecules*, 1972, 5: 171–177

19 Brown EV, Granneman GR. *Cis-tran*s isomerism in pyridyl analogs of azobenzene. Kinetic and molecular-orbital analysis. *J Am Chem Soc*, 1975, 97: 621–627

20 Nerbonne JM, Weiss RG. Elucidation of thermal-isomerization mechanism for azobenzene in a cholesteric liquid-crystal solvent. *J Am Chem Soc*, 1978, 100: 5953–5954

21 Haitjema HJ, Tan YY, Challa G. Thermal isomerization of azobenzene-based acrylic-monomers and (co)polymers with dimethylamino substituents in solution, influence of addition of (poly)acid, copolymer composition, spacer length, and solvent type. *Macromolecules*, 1995, 28: 2867–2873

22 Wei WH, Tomohiro T, Kodaka M, Okuno H. Selective synthesis and kinetic measurement of 1:1 and 2:2 cyclic compounds containing 1,4,7,10-tetraazacyclododecane and azobenzene units. *J Org Chem*, 2000, 65: 8979–8987

23 Wang CH, Weiss RG. Thermal *cis*→*trans* isomerization of covalently attached azobenzene groups in undrawn and drawn polyethylene films. Characterization and comparisons of occupied sites. *Macromolecules*, 2003, 36: 3833–3840

24 Tamaoki N, Yamaoka T. Light-intensity dependence in the photochromism of dibenzo[2.2](4.4′)-azobenzenophane. *J Chem Soc Perk T 2*, 1991, 6: 873–878

25 H. Rau, D. Röttger, Photochromic azobenzenes which are stable in the *trans* and *cis* forms. *Mol Cryst Liq Cryst Sci Technol A*, 1994, 246: 143–146

26 Schmiegel J, Grutzmacher HF. A macrocyclic 2,19-dioxo[3.3](3,3′) azobenzolophane by transition-metal carbonyl complex-mediated CO insertion and cyclization. *Chem Ber*, 1990, 123: 1749–1752

27 Nagamani SA, Norikane Y, Tamaoki N. Photoinduced hinge-like molecular motion: Studies on xanthene-based cyclic azobenzene dimers. *J Org Chem*, 2005, 70: 9304–9313

28 Norikane Y, Katoh R, Tamaoki N. Unconventional thermodynamically stable *cis* isomer and *trans* to *cis* thermal isomerization in reversibly photoresponsive [0.0](3,3′)-azobenzenophane. *Chem Commun*, 2008: 1898–1900

29 Ortruba JP, Weiss RG. Liquid Crystalline Solvents as Mechanistic Probes. 11. The *syn*→*anti* thermal isomerization mechanism of some low-“bipolarity” azobenzenes. *J Org Chem*, 1983, 48: 3448–3453

30 Rau H, Shen YQ. Photoisomerization of sterically hindered azobenzenes. *J Photochem Photobiol A: Chem*, 1988, 42: 321–327

31 Wheeler OH, Gore PH. Absorption spectra of aromatic azo and related compounds. IV. Benzanils. *J Org Chem*, 1961, 26: 3295–3301

32 Forber CL, Kelusky EC, Bunce NJ, Zerner MC. Electronic spectra of *cis*-azobenzenes and *trans*-azobenzenes: consequences of ortho substitution. *J Am Chem Soc*, 1985, 107: 5884–5890

33 Bunce NJ, Ferguson G, Forber CL, Stachnyk GJ. Sterically hindered azobenzenes: Isolation of *cis* isomers and kinetics of thermal *cis-trans* isomerization. *J Org Chem*, 1987, 52: 394–398

34 Han M, Ishikawa D, Honda T, Ito E, Hara M. Light-driven molecular switches in azobenzene self-assembled monolayers: Effect of molecular structure on reversible photoisomerization and stable *cis* state. *Chem Commun*, 2010, 46: 3598–3600

35 Han M, Hirade T, Hara M. A reversibly photoswitchable mononuclear palladium(II) complex with ortho-diethylated azobenzene ligands. *New J Chem*, 2010, 34: 2887–2891

36 Tamada K, Akiyama H, Wei TX, Kim SA. Photoisomerization reaction of unsymmetrical azobenzene disulfide self-assembled monolayers: Modification of azobenzene dyes to improve thermal endurance for photoreaction. *Langmuir*, 2003, 19: 2306–2312

37 For instance, solubility of **7p** in DMF is < 0.1 mg/1mL

38 Gabe EJ, Wang Y, Barclay LRC, Dust JM. Structures of hindered azobenzenes. 3. 2,2′,4,4′,6,6′-Hexamethylazobenzene. *Acta Crystallogr B*, 1981, 37: 978–979

39 Han MR, Hashizume D, Hara M. 1-[(*E*)-3-sec-butyl-4-(4′-ethoxy-3,5-diethylbiphenyl-4-yldiazenyl)phenoxy]hexadecane. *Acta Crystallogr E*, 2006, 62: O3001–O3003

40 Han M, Ichimura K. Tilt orientation of *p*-methoxyazobenzene side chains in liquid crystalline polymer films by irradiation with nonpolarized light. *Macromolecules*, 2001, 34: 82–89

41 Tamada K, Nagasawa J, Nakanishi F, Abe K, Ishida T, Hara M, Knoll W. Structure and growth of hexyl azobenzene thiol SAMs on Au(111). *Langmuir*, 1998, 14: 3264–3271

HAN Mina was born in Gyeonggi-do, Korea, received her B.S. degree in Chemistry Education from Kongju National Teachers University and her M.S. degree in Chemistry from Yonsei University. In 1997, she joined Professor Kunihiro Ichimura’s group at Tokyo Institute of Technology in Yokohama, obtaining her Ph.D. in 2000 in the area of photofunctional organic materials and liquid crystalline polymers. She undertook a postdoctoral research with Professor Georges Belfort at Rensselaer Polytechnic Institute from 2001 to 2003, and then moved to RIKEN as a Japan Society for the Promotion of Science (JSPS) fellow. In 2008, she returned to Tokyo Institute of Technology, where she is currently an assistant professor of Chemistry and Electronic Chemistry. Her research interests include photochromic materials, self-assembly, organic nano/micro-structured materials.

HONDA Takumu was born in Fukushima Prefecture, Japan, in 1984. He received his B.S. degree (2007) in applied chemistry from Shibaura Institute of Technology and his M.S. degree (2009) in electronic chemistry from Tokyo Institute of Technology, where he worked on the synthesis and characterization of photofunctional organic materials. He is currently a researcher at Kansai Paint Co., Ltd., Japan.